Effect of Short-Chain Branching on the Rheology of Polyolefins

César A. García-Franco,*,† Bruce A. Harrington,† and David J. Lohse‡

ExxonMobil Chemical Co., Baytown Technology & Engineering Complex/West, 5200 Bayway Dr., Baytown, Texas 77522, and ExxonMobil Research & Engineering Co., Corporate Strategic Research Labs., 1545 Route 22 East, Annandale, New Jersey 08801

Received December 2, 2005; Revised Manuscript Received January 31, 2006

ABSTRACT: A series of carefully synthesized ethylene/butene copolymers (0.2−0.85 mole fraction butene) were synthesized using metallocene catalysts to probe the relationship between the chemical architecture of polyolefins and their rheology. The dependence of G_N^0, the plateau modulus, on m_b, the molecular weight per backbone bond, which we have seen previously for polyolefins is obeyed by these copolymers. Moreover, the modulus at the frequency at which $G' = G''$ also scales with copolymer composition. We also show that the van Gurp−Palmen plots ($|G^*|$ vs δ) for these copolymers show a universal behavior, which could allow for the characterization of copolymer composition by rheology. We demonstrate that combining small-amplitude oscillatory shear data with stress relaxation experiments the theory of linear viscoelasticity allows us to determine low-frequency behavior much more rapidly. The zero shear viscosity of these ethylene copolymers also shows a regular dependence on the copolymer composition, and we propose a new scaling relationship for zero shear viscosity in terms of m_b. We show that this applies to a wide range of polyolefins and show similar relations for the equilibration time, τ_e, and monomeric friction factor, ζ.

Introduction

On the Plateau Modulus, G_N^0. A fundamental viscoelastic material function is the modulus associated with the rubbery plateau, G_N^0, exhibited by polymer melts. According to the theory of rubber elasticity, the plateau modulus is defined by the following equation

$$G_N^0 = \frac{\beta \rho RT}{M_e} \tag{1}$$

where R is the ideal gas constant, T is the absolute temperature, M_e is the entanglement molecular weight, and the coefficient β according to Ferry[1] is equal to 1 and according to Doi and Edwards[2] is equal to 4/5. (See Larson et al.[3] for a good discussion concerning the value of β.)

In the theory of reptation,[2] entanglement spacing is not specified. The tube diameter proves to be an equivalent parameter. M_e affects the rubbery and terminal zone of polymer melts. The importance of M_e is reflected by the fact that it has strong consequences on both viscous and elastic properties.[1,2,4] M_e has also been reported to affect the micromechanisms of deformation (crazing and shear yielding) and the failure of polymers in the solid state.[5−9]

A comprehensive review of methods proposed in the literature to calculate G_N^0 from rheological data has been made,[10] in connection to the rheology of ethylene/octene copolymers. We will follow those procedures herein.

Relating Plateau Modulus to Chemical Structure. A key goal of polymer science has been to relate the chemical structure of macromolecules to their basic physical properties. The packing length model has proved successful at predicting the degree of entanglement of flexible polymers based on their chain dimensions and density.[11] We have recently[12] extended this further for polyolefins by connecting their chemical architecture to the packing length and so to the plateau modulus.

The packing length is defined as

$$p = \frac{M}{\rho N_A \langle R^2 \rangle_0} \tag{2}$$

where $\langle R^2 \rangle_0$ is the mean-square end-to-end distance of a chain, M is the molecular weight of the polymer, ρ is its density, and N_A is Avogadro's number. This parameter is an intrinsic characteristic of a polymer that is independent of molecular weight, and we have shown that it directly controls the degree to which the chains entangle. So it gives a good model for predicting the plateau modulus of polymers from their chain dimensions.

The simplest model for the packing length of polyolefin chains is the "backbone equivalence" model, which states that the size of a coil is determined just by the contour length of the backbone. This is the same as assuming that the ratio of trans to gauche configurations is the same for all polyolefins as it is for polyethylene. For the plateau modulus this leads to the following prediction:

$$G_N^0 = \left(\frac{14}{m_b}\right)^3 (G_N^0)_{PE} \tag{3}$$

where m_b is the molecular weight per backbone bond and $(G_N^0)_{PE}$ is the plateau modulus of polyethylene.

However, we[12] have shown that the backbone equivalence model, while capturing the qualitative drop of G_N^0 with increasing comonomer content and length, does not predict the plateau modulus quantitatively. By fitting the data on polyolefins, we derived the following equations for the plateau modulus at 190 °C, depending on the value of m_b:

$$G_N^0 = 24820 m_b^{-3.49} \quad (m_b = 14-28 \text{ g/mol}) \tag{3a}$$

and

$$G_N^0 = 41.84 m_b^{-1.58} \quad (m_b = 35-56 \text{ g/mol}) \tag{3b}$$

† ExxonMobil Chemical Co.
‡ ExxonMobil Research & Engineering Co.

10.1021/ma052581o CCC: $33.50
Published on Web 03/01/2006

Table 1. Laboratory and Commercial Ethylene−Butene Copolymers[a]

polymer[d]	*mf*	*wf*	M_w (kg/mol)	M_w/M_n (DRI)	M_z/M_w (MALLS)	G_{co} (kPa)	G_N^0 (kPa)	m_b (g/mol)	η_0 (kPa s)	M_e (kg/mol)	τ_e (ns)	ζ (Nns/m)
EB07[c]	0.038	0.073	111	2.29	2.99	166	2180[c]	14.5	3.4	1.08	2.82E+0[e]	5.78E−4
EB11[c]	0.058	0.109	115	2.21	1.72	113	2040[c]	14.8	3.2	1.15	3.15E+0	5.90E−4
EB19[c]	0.104	0.189	144	2.23	1.58	93.1	1756[c]	15.5	8.2	1.34	7.27E+0	1.11E−3
EB23[c]	0.128	0.227	89	2.35	2.07	173	1631[c]	15.8	1.7	1.44	1.07E+1	1.47E−3
EB26[c]	0.151	0.263	75	2.16	1.79	165	1517[c]	16.1	0.76	1.55	1.18E+1	1.47E−3
EB33[e]	0.196	0.328	209	1.82		178	1210[b]	16.7	38.9	1.95	5.01E+1	4.43E−3
EB65[e]	0.476	0.645	387	2.10	1.54	85.0	529[b]	20.7	58.6	4.45	3.54E+2	9.77E−3
EB66[e]	0.493	0.66	356	2.06	1.54	67.0	445[b]	20.9	33.2	5.29	5.70E+2	1.19E−2
EB75[e]	0.593	0.745	351	1.98	1.45	68.9	436[b]	22.3	23.1	5.40	4.55E+2	9.81E−3
EB77[e]	0.628	0.771	915	2.05	1.36	64.8	456[b]	22.8	694	5.17	4.32E+2	1.03E−2
EB87[e]	0.764	0.866	810	1.99	1.41	48.9	356[b]	24.7	246	6.62	6.89E+2	1.17E−2
EB92[e]	0.847	0.917	761	2.17	1.42	38.8	286[b]	25.9	154	8.24	1.40E+3	1.73E−2

[a] *mf* = C_4 mole fraction, *wf* = C_4 weight fraction, M_w = measured with MALLS, C_{co} = crossover modulus, η_0 = zero shear viscosity measured at 190 °C, and m_b = molecular weight per backbone bond. [b] Plateau modulus calculated from experimental data by the integration of the $G''-\omega$ dispersion. [c] Calculated according to the power law models; eq 3a. [d] c = commercial polymer; e = experimental polymer. [e] Read as 2.82×10^0.

The physics behind these relations is not known, beyond indicating that the gauche/trans ratio depends on m_b. The reasons for this are currently being studied. In this paper we study a carefully prepared set of ethylene/butene copolymers to see how well this model holds up over a broad range of composition. The results clearly show the strong effect of comonomer content on the plateau modulus. We then proceed to show how other rheological properties depend on copolymer composition.

Experimental Section

General Polymerization Procedure. For the laboratory-produced copolymers the process conditions and reagents were chosen specifically to minimize branching, molecular weight distribution, and composition distribution. Thus, all reactions were carried out in a single-phase, liquid-filled, stirred tank reactor with continuous flow of feeds to the system and continuous withdrawal of products under equilibrium conditions. All polymerizations were done in a hexanes solvent system using soluble, single-sited, ansa-metallocene and soluble, discrete, noncoordinating borate anions as cocatalysts. A homogeneous dilute solution of tri-*n*-octylaluminum in hexane was used as a scavenger in the minimum allowable concentration needed to maintain reaction. In addition, the polymerizations were carried out at reasonably low temperatures using hydrogen to control molecular weight. In this manner it was possible to minimize misinsertions and macromer reinsertions that can contribute to long-chain branching. This combination of low-temperature, homogeneous solution process conditions and single-sited catalysts and activators helped to ensure that the products were as narrowly dispersed, and as linear as possible, with metallocene copolymerizations.

Polymerization Example. Using the general processes described above, a series of model ethylene−butene polymerizations were carried out by varying monomer feed ratios. The details for the polymerization of EB92 follow:

Catalyst Activation. μ-(*p*-$Et_3SiPh)_2C(Cp)(2,7di$-*t*-BuFlu)$HfMe_2$ (82.5 mg, 0.0872 mol) was preactivated with *N*,*N*′-dimethylanilinium tetrakis(perfluorophenyl)borate [$DMAH^+B(pfp)_4^-$] (67.5 mg, 0.0843 mmol) in toluene (900 mL) under an inert atmosphere. This mixture was allowed to activate until the evolution of methane stopped and the solution was clear and then was sealed with nitrogen pressure for transfer to a delivery vessel. The catalyst solution was pumped to the reactor from the delivery vessel at a controlled rate using a calibrated HPLC pump.

Copolymer Synthesis. A mixture of chilled hexanes (5.4 L/h) was pumped into a 1 L, liquid-filled, stirred tank reactor while the reactor temperature was held constant using a steam/water mixture flowing through the reactor jacket. The preactivated catalyst in toluene (0.090 L/h, 0.0073 mmol/h) and a scavenger solution of tri-*n*-octylaluminum in hexane (0.090 L/h, 0.3226 mmol/h) were then pumped to the reactor for 20 min before monomers were introduced. 1-Butene (0.675 L/h, 6.51 mol/h) was pumped to the chilled feed line as a liquid. Ethylene was delivered as a gas in a controlled fashion through a mass flow meter/controller (18.0 g/h, 0.643 mol/h) and dissolved in the chilled solvent before entering the reactor. Hydrogen gas was delivered to the chilled feed line in a controlled manner through a mass flow meter/controller (0.0032 g/h, 179 ppmw on ethylene) as needed for molecular weight control. Continuous flow was established at a constant temperature (60 °C) and stirring rate (∼1550 rpm). Onset of polymerization activity was determined by an observation of a viscous product and reduced steam heat needed to control reactor temperature. Once activity was established, 1.5 h was provided to establish equilibrium conditions. The resulting mixture, containing mostly solvent, polymer (1.8 wt %), and unreacted monomers, was collected (0.5 h) in a vessel containing an alcohol to quench the polymerization activity. A stabilizer was added to the polymer solution and mixed. The solvent was evaporated on a steam bath and the product dried under vacuum at 90 °C for 16 h. The resulting solid (25 g) was analyzed for composition by ^{13}C NMR (91.7 wt % butene) and for molecular weight by GPC (760 kg/mol $M_{w,Malls}$ and $MWD_{DRI/DRI}$ = 2.17).

Table 1 summarizes the product properties for this series of ethylene−butene plastomers and also provides data of selected commercial C_2/C_4 copolymers.

Small-Amplitude Oscillatory Shear and Stress Relaxation Rheology. Mechanical spectroscopy in the frequency domain (small-amplitude oscillatory shear experiment) was employed to measure the linear viscoelastic properties of these copolymers. All dynamic rheological experiments were performed using a stress-controlled instrument MCR 500 (Paar-Physica) with parallel plates (25 mm diameter) geometry. To minimize thermally induced chemical changes, the experimental specimens were kept in a nitrogen atmosphere during the rheological test. The experimental specimens were stabilized and compression-molded at 190 °C, with a diameter of 25 mm and a thickness of ∼1 mm. The dynamic experiments were carried out at 190 °C using a harmonic stress of amplitude equal to 1 kPa. A typical dynamic spectrum corresponding to copolymer EB87 is shown in Figure 1.

The linear viscoelastic properties of these experimental ethylene/butene copolymers were also measured in the time domain at 190 °C using a step strain experiment with a strain of 10%.

Results

Effect of Butene Content on the Plateau Modulus. The dynamic data at 190 °C were employed to calculate G_N^0 of these ethylene/butene copolymers. The rubbery plateau modulus was calculated using the following four methods: (i) Integration of the $G''(\omega)-\omega$ dispersion, using both a Gaussian extrapolation and a straight line extrapolation to high frequencies;[10] (ii) according to the theory of Marvin−Oser[13,14] and Carri−Winter[15] relationship, predicated on the maximum exhibited by $G''(\omega)$; (iii) using the crossover modulus and polydispersity according

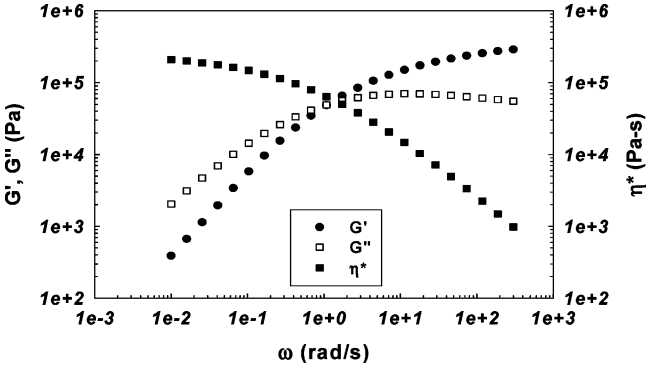

Figure 1. Typical dynamic moduli spectrum. Copolymer EB87 at 190 °C.

Table 2. Summary of the Plateau Modulus

material	G_N^0 (kPa)[a]	G_N^0 (kPa)[b]	G_N^0 (kPa)[c]	G_N^0 (kPa)[d]	G_N^0 (kPa)[e]
EB33	1210	1226	1300	1120	1182
EB92	286	293	270	284	283
EB77	456	468	433	453	455
EB87	356	385	338	333	340
EB65	529	id	570	607	545
EB75	436	id	488	468	486
EB66	445	id	488	471	530

[a] Integration of the $G''-\omega$ dispersion:[1] $G_N^0 = (2/\pi)\int_{-\infty}^{\infty} G''(\omega)\, d \ln \omega$. Gaussian extrapolation. [b] Integration of the $G''-\omega$ dispersion:[1] $G_N^0 = (2/\pi)\int_{-\infty}^{\infty} G(\omega)\, d \ln \omega$. Straight line extrapolation. id: insufficient data. [c] Marvin−Oser[14,15] theory (also the Carri and Winter[16] method): $G_N^0 = 4.83 G_{max}$. [d] Wu[17,18] method: $\log(G_N^0/G_{co}) = 0.38 + [2.63 \log(M_w/M_n)]/[1 + 2.45 \log(M_w/M_n)]$. [e] Wu,[17] Onogi,[19] Masuda;[20] $G_N^0 = (4/\pi)\int_{-\infty}^{\omega_{max}} G\, d \ln(\omega)$.

to the Wu[16,17] method; and (iv) integration of the $G''(\omega)-\omega$ dispersion from $-\infty$ to the frequency, ω_∞, at which G'' exhibits a maximum and multiplying the result by 2.[16,18,19] A summary of the plateau modulus calculated by these four methods is given in Table 2. For the five polymers with the highest ethylene content we were not able to determine G_N^0 by any of these methods due to the onset of crystallization at low temperatures. Therefore, we calculated G_N^0 according to eq 3a.

The predictions of the backbone equivalence model (eq 3) and the power law model (eqs 3a and 3b) contrasted with the experimentally obtained plateau modulus of these C_2/C_4 copolymers are given in Figure 2. A cursory review of these data shows an excellent agreement between the power law model predictions and the experimentally observed plateau modulus of these copolymers. The good agreement of the calculated values of G_N^0 according to different methods is also evident. In the remainder of the report, we will use the value of the plateau modulus calculated by the integration of the $G''-\omega$ dispersion.

Van Gurp−Palmen Plots. The Van Gurp−Palmen[20−22] plots of these C_2/C_4 copolymers based on the linear viscoelastic measurements at 190 °C are shown in Figure 3. As a reference, the plot also shows the evolution of the phase angle, δ, in terms of $|G^*|$ of a linear monodisperse hydrogenated polybutadiene (PEL 193). This representation of the linear viscoelastic properties is molecular weight and temperature invariant; however, it is very sensitive to polydispersity and the presence of long-chain branching. In the present case, δ shows a strong dependence on the comonomer content. As butene content increases, the entire curve shifts down toward the left on the modulus axis, as was the case with octene copolymers.[10] The value of G_N^0 is approximated by these curves at the lower limit of δ and can be estimated by a modest extrapolation. Therefore,

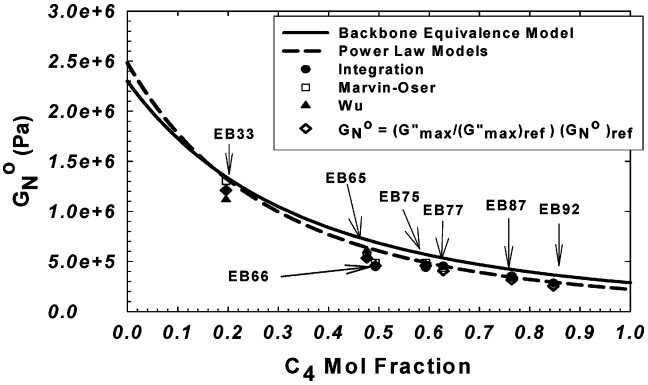

Figure 2. Comparison of the plateau modulus predictions of the backbone equivalence model (eq 3) and power law models (eq 3a) against the experimental values of the plateau modulus calculated according several methods: (i) integration of the G'' dispersion, (ii) according to the Marvin−Oser equation, (iii) according to Wu's equation, and (iv) according to $G_N^0 = (G''_{max}/(G''_{max})_{ref})(G_N^0)_{ref}$. Excellent agreement is obtained between the power law models and experimental values of the rubbery plateau modulus.

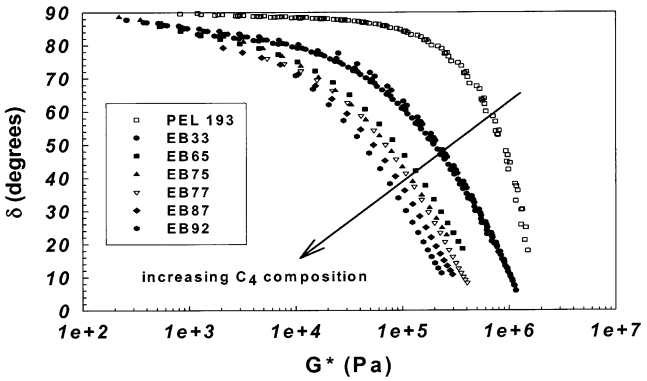

Figure 3. Van Gurp−Palmen plots, phase angle, δ, vs $|G^*|$ of experimental C_2/C_4 copolymers; linear monodisperse hydrogenated polybutadiene PEL193 is included as reference.

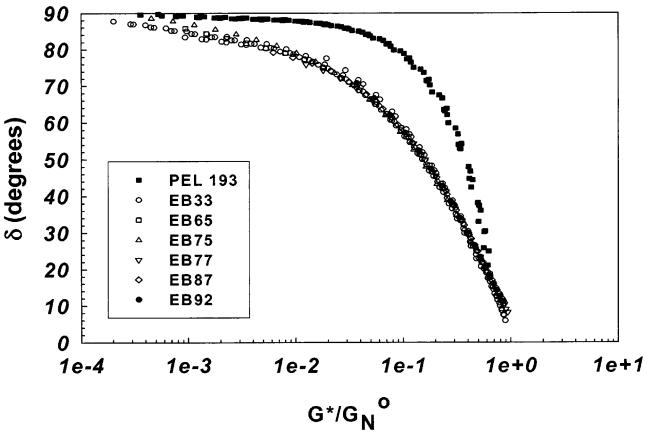

Figure 4. Normalization of the absolute value of the complex modulus by the plateau modulus removes the effect of comonomer content on the Van Gurp−Palmen plot. Monodisperse linear hydrogenated anionically polymerized polybutadiene (PEL 193) is included as a reference.

the Van Gurp plots can be used to estimate G_N^0. This dependence of the Van Gurp−Palmen plots on the copolymer composition provides a means to estimate the rubbery plateau modulus and the copolymer composition in a high throughput experimentation environment.

Figure 4 shows the behavior of the phase angle, δ, as a function of the normalized absolute value of the complex

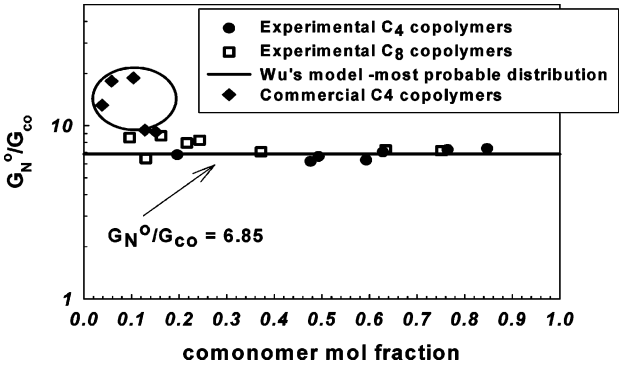

Figure 5. Normalized plateau modulus (G_N^0/G_{co}) of experimental C_2/C_4, C_2/C_8, and commercial C_2/C_4 copolymers against comonomer content. Wu's model for most probable MWD predicts $G_N^0/G_{co} = 6.85$.

modulus, i.e. $|G^*|/G_N^0$. This normalization causes the different curves to collapse onto a single one regardless of the comonomer content over the entire normalized modulus axes. The difference between the linear nearly monodisperse anionically polymerized PEL193 (model C_2/C_4 polymer with ca. 8 wt % butene) and the metallocene-catalyzed C_2/C_4 with $M_w/M_n \approx 2$ is due to molecular weight distribution effects.

Crossover Modulus G_{co}. As stated earlier, the crossover modulus ($G_{co} = G' = G''$) is a useful parameter in the rheological characterization of polymer melts, it exhibits a strong dependence on the molecular weight distribution, and it is a weak function of the molecular weight and temperature. It is of interest to investigate the effect of composition on this parameter. The crossover moduli of these ethylene−butene copolymers are given in Table 1. Since these C_2/C_4 copolymers are relatively narrow and similarly dispersed (close to a most probable distribution), we should observe a relationship between the crossover modulus and the copolymer composition.

As can be seen in Table 1, the crossover modulus scales with the butene mole fraction of the copolymer. Thus, the crossover modulus can be used also as a fast rheological means to determine the composition of metallocene copolymers. However, if the molecular weight is too high or too low, G_{co} might not be observed in the experimentally accessible frequency window.

The model proposed by Wu[16,17] correlates the plateau modulus, G_N^0, the crossover modulus, G_{co}, and the polydispersity, M_w/M_n. For a most probable distribution this model predicts $G_N^0/G_{co} = 10^{0.8356} = 6.85$. Therefore, this ratio is independent of the copolymer composition.

Figure 5 shows a plot of G_N^0/G_{co} vs the comonomer composition of the experimental butene and octene copolymers as well as the commercial ethylene/butene copolymers. For the butene copolymers ratio G_N^0/G_{co} is independent of the butene mole fraction, and it is very close to the predicted value of a most probable distribution. Four C_2/C_8 copolymers show a good agreement with the value predicted by Wu's model for a most probable distribution. The remaining four C_2/C_8 copolymers, toward the low end of the composition, deviate from the 6.85 value with an average deviation of ca. 12%. Figure 5 also shows the G_N^0/G_{co} ratio of commercial C_2/C_4 copolymers. EB07, EB11, and EB19 clearly do not follow a most probable molecular weight distribution, whereas EB23 and EB26 show similar deviations from 6.85 as some of the C_2/C_8 copolymers.[10]

Stress Relaxation. Step strain experiments (stress relaxation) were performed with the MCR-500 rheometer at 190 °C using 10% strain and parallel plate geometry. The weight-average molecular weight seems to control the relaxation. For example,

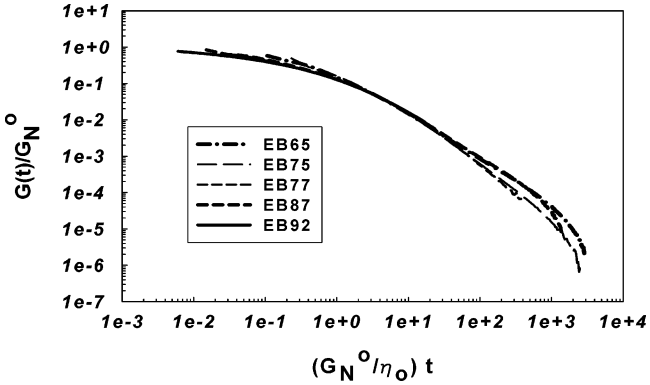

Figure 6. Normalized relaxation function against normalized time achieves the superposition of the relaxation modulus curves.

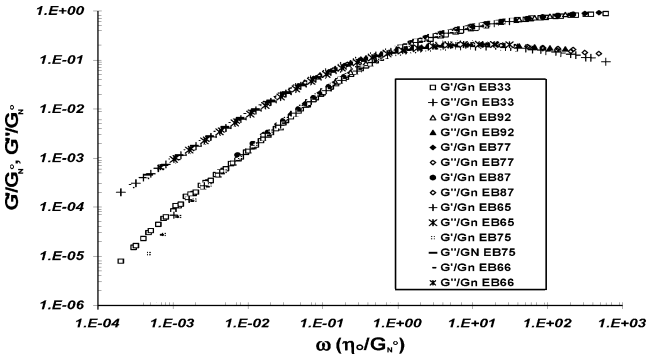

Figure 7. Normalization of the dynamic moduli and the frequency achieves superposition of the experimental data regardless of molecular weight and comonomer composition for these experimental C_2/C_4 copolymers.

the copolymer EB75 ($M_w = 351$ kg/mol) displays the fastest relaxation, whereas the copolymer EB77 ($M_w = 915$ kg/mol) shows the slowest relaxation. The comonomer composition does not seem to influence the relaxation over the experimentally accessible time.

The relaxation data of some of these ethylene/butene copolymers in terms of normalized axes are presented in Figure 6. The relaxation modulus, $G(t)$, has been normalized by the corresponding value of the plateau modulus, G_N^0, and the time axis by the number-average relaxation time. The number-average relaxation time (first-order moment of the normalized relaxation spectrum) is defined in terms of the relaxation spectrum, $H(\lambda)$, as

$$\langle\lambda\rangle_n = \frac{\eta_0}{G_N^0} = \frac{\int \lambda H(\lambda)\, \mathrm{d}\ln\lambda}{\int H(\lambda)\, \mathrm{d}\ln\lambda} \tag{4}$$

Figure 6 shows that as a consequence of this normalization procedure all the relaxation curves merge onto a universal one regardless of their molecular weight and comonomer composition of these copolymers, emphasizing the fundamental character of the plateau modulus and the zero shear viscosity.

It is useful and of considerable interest to achieve such a superposition with the linear viscoelastic properties measured in the frequency domain such as the dynamic moduli ($G'(\omega)$, $G''(\omega)$).

Figure 7 shows a plot of the dynamic moduli normalized by the plateau modulus against the angular frequency normalized by the reciprocal of the number-average relaxation time $\omega\eta_0/G_N^0$. These normalizations yields a remarkable superposition of the storage modulus, G', and the loss modulus, G'', onto a single

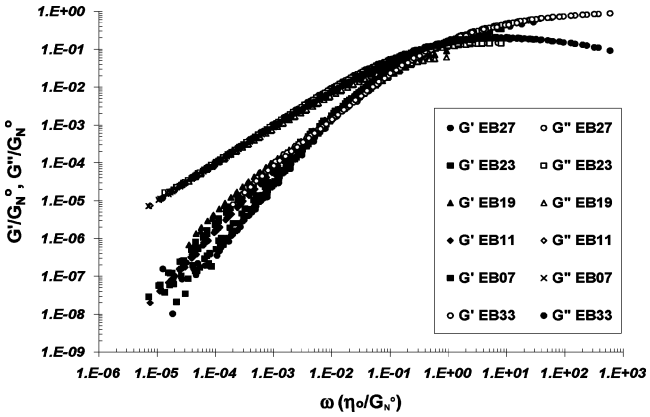

Figure 8. Normalized moduli plotted against normalized frequency of commercial and experimental copolymers. EB33 is representative of the experimental copolymers. Effects of molecular weight distribution are evident on the value of G'/G_N^0 at low frequencies. Broadening of the MWD prevents superposition at low frequencies.

"universal" curve regardless the molecular weight and composition of these copolymers, implying a universality in the long relaxation processes of flexible entangled polymers.

A similar plot, including the commercial copolymers, is shown in Figure 8. EB33 is included as a representative of the experimental copolymers which has been shown to superpose with the other experimental copolymers. These data show that the superposition of the commercial copolymers is not as perfect as the superposition achieved by the experimental ones. The major difficulty is the superposition of the normalized storage modulus, G'/G_N^0, at low frequencies, and also some superposition difficulties are detected in the crossover region of the normalized moduli. These problems can be traced to the broader molecular weight distribution of these commercial copolymers.

Zero Shear Viscosity. The zero shear viscosities of these experimental C_2/C_4 copolymers and some commercial C_2/C_4 copolymers were measured at 190 °C and are reported in Table 1. The zero shear viscosities of linear and narrowly dispersed polyethylene scale with an exponent close to the 3.4 power of the weight-average molecular weight. On the basis of hydrogenated anionically polymerized polybutadiene, we have found the following relationship between the zero shear viscosity in Pa·s and the weight-average molecular weight at 190 °C.[23]

$$\eta_0 = 6.04 \times 10^{-14} M_w^{3.33} \quad (5)$$

We note that this equation has been found not only from extensive experimentation but also from some simulations.[24] As earlier stated, these linear model polyethylenes (hydrogenated anionically polymerized polybutadienes) are analogous to C_2/C_4 copolymers with an average comonomer content of ca. 8 wt %.

Figure 9 shows the zero shear viscosity of these commercial and experimental ethylene−butene copolymers as a function of the weight-average molecular weight as well as the $\eta_0 \propto M_w^{\alpha}$ relationship based upon the linear model polyethylenes (eq 5). The zero shear viscosities of the commercial ethylene/butene copolymers with comonomer incorporation ranging from 7.3 to 32.8 wt % fall on the model polyethylenes (ca. 8 wt % butene) correlation. On the other hand, the viscosities of the experimental copolymers with considerably higher butene content (65−92 wt %) fall beneath the model polyethylene correlation. This is a consequence of comonomer effect on the plateau modulus. Therefore, the zero shear viscosity of ethylene/α-olefin copolymers depends on the amount of incorporated comonomer.

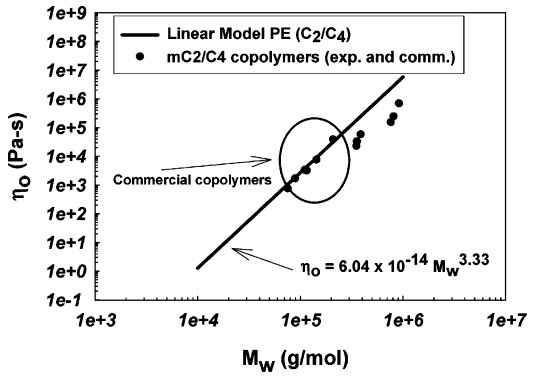

Figure 9. Zero shear viscosity of experimental and commercial C_2/C_4 copolymers compared to the scaling relationship for linear monodisperse copolymers given by eq 5.

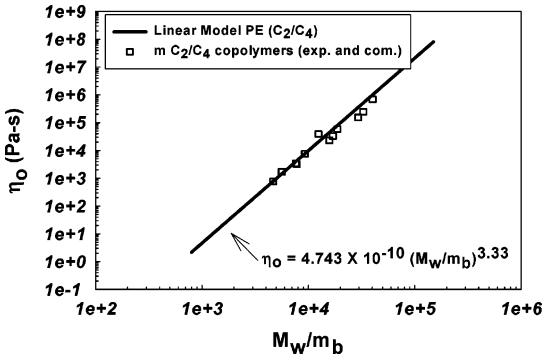

Figure 10. Zero shear viscosity of experimental and commercial C_2/C_4 copolymers as a function of the normalized weight-average molecular weight. M_w/m_b removes the effect of comonomer content on the zero shear viscosity.

It is of considerable practical and fundamental interest to remove the comonomer effect on the zero shear viscosity. This is accomplished by using the molecular weight per backbone bond, m_b, as a normalizing variable of the weight-average molecular weight. Figure 10 shows the zero shear viscosity of these experimental and commercial ethylene/butene copolymers against the normalized molecular weight, M_w/m_b. This plot also contains the scaling relationship of the model polyethylenes (eq 6) in terms of the normalized molecular weight (M_w/m_b):

$$\eta_0 = 4.743 \times 10^{-10} \left(\frac{M_w}{m_b}\right)^{3.33} \quad (6)$$

It is evident from the data shown in Figure 10 that the normalization of M_w using m_b (which depends only on the chemical structure of the copolymer) does remove the comonomer effect on the zero shear viscosity of these ethylene copolymers. We have also decided to include in this analysis some other data from the literature. First is the rheology on a set of metallocene polymers reported by Miyata et al.[25] These were mostly ethylene−hexene copolymers over a broad range of compositions as well as one ethylene−propylene copolymer. These data are listed in Table 3. We also include the extensive set of data on hydrogenated polybutadienes that was reported by Carella et al.[26] These were based on the saturation of polybutadienes that had been synthesized by anionic techniques to have nearly polydispersities very close to one and a range of vinyl contents. Once saturated, these give a set of nearly monodisperse saturated polymers that have a structure identical to ethylene−butene random copolymers. Their data are given in Table 4, where we show the composition in equivalent butene weight fraction (which is simply equal to the fraction of vinyl

Table 3. Ethylene−Hexene and Ethylene−Propylene Copolymers

copolymer	*mf*	*wf*	M_w (kg/mol)	M_w/M_n (DRI)	G_N^0 (kPa)	m_b (g/mol)	η_0 (kPa·s)	M_e (kg/mol)	τ_e (ns)	ζ (Nns/m)
EP37	0.372	0.47	102	1.44	1060	16.6	2.728	2.22	7.20E+01	5.08E−03
EH25	0.252	0.503	145	1.41	600	21.1	3.666	3.93	3.58E+02	1.24E−02
EH33	0.334	0.601	202	1.46	420	23.4	6.11	5.61	9.29E+02	1.97E−02
EH40	0.398	0.665	248	1.64	440	25.1	5.289	5.35	3.26E+02	8.04E−03
EH51	0.505	0.754	231	1.67	310	28.1	1.942	7.60	7.12E+02	1.10E−02

Table 4. Hydrogenated Polybutadienes

copolymer	*mf*	*wf*	M_w (kg/mol)	G_N^0 (kPa)	m_b (g/mol)	η_0 (kPa·s)	M_e (kg/mol)	τ_e (ns)	ζ (Nns/m)
HPB15	0.08	0.145	171	2050	15.1	24	1.14	5.87E+00	1.14E−03
HPB20	0.11	0.195	181	1810	15.5	25.7	1.29	8.99E+00	1.45E−03
HPB26	0.15	0.255	186	1550	16.0	37.8	1.51	2.40E+01	3.09E−03
HPB30	0.18	0.3	82	1390	16.5	1.25	1.69	2.09E+01	2.30E−03
HPB35	0.21	0.35	190	1250	17.0	36.3	1.89	5.62E+01	5.32E−03
HPB40	0.25	0.4	174	1070	17.5	19	2.21	7.89E+01	5.95E−03
HPB43	0.27	0.425	79	1100	17.8	1	2.15	5.39E+01	4.32E−03
HPB99	0.98	0.99	360	200	27.7	3.63	12.06	2.19E+03	1.57E−02

incorporation in the parent polybutadiene). The zero shear viscosities of these polymers have been plotted in Figure 11 and compared to eq 6, which does a good job of describing all of these data. This fact underlines once more the fundamental character of the molecular weight per backbone bond concept.

Equilibration Time and Monomeric Friction Factor. The fact that we have seen a correlation between the zero shear viscosity, η_0, and a parameter based on the chemical nature of these copolymers, m_b, has some profound implications. This gives us hope that we might begin to make a connection between the chemical makeup of a polymer and the basic parameters that set the time scale for the relaxation of the chains. These are usually represented in terms of the equilibration time, τ_e, or the monomeric friction factor, ζ, which are described below. The realization of such a connection would provide us with a very powerful tool for polymer rheology. Given values of τ_e and M_e (or equivalently G_N^0), one can predict the linear viscoelasticity of any polymer, regardless of molecular weight distribution, through the use of the double-reptation model for an assembly of linear chains.[27] Such a predictive power would allow us to connect the chemistry of a polymer directly to its rheology, and vice versa.

Models. The equilibration time, τ_e, is the Rouse relaxation time of a chain of length M_e, and from it one can calculate all of the relevant times associated with the reptation model of polymer flow.[2,3] The various models for constraint release and double reptation give slightly different expressions for relating τ_e to η_0, and van Meerveld[28] has recently reviewed these. He shows that the following expression, based on the models of Likhtman and McLeish,[29] gives the best fit for a number of polymers

$$\eta_0 = 0.064\tau_e \frac{\rho RT}{M_e}(M/M_e)^{3.4} \tag{7}$$

where a value of $\beta = {}^4/_5$ is used in eq 3 of ref 4 to define M_e. When values of η_0, M_e, and M have been measured for a polymer, it is clear that eq 7 can be used to extract a value of τ_e.

The monomeric friction factor ζ was first defined by Ferry[1] and is meant to represent the energy needed for one repeat unit to make one "step" in some dynamic process. As such, it can be related to either the diffusion or viscosity, especially for small, nonentangled molecules. For high-molecular-weight entangled polymers, τ_e and ζ can be related by[3]

$$\tau_e = \left(\frac{M_e}{m_0}\right)\frac{\zeta M_e[\langle R^2\rangle_0/M]}{3\pi^2 k_B T} = \left(\frac{M_e}{m_0}\right)\frac{\zeta M_e}{3\pi^2 \rho RTp} \tag{8}$$

In eq 8, m_0 is the molecular weight of the monomer unit used to define ζ. This can be problematical to define since we do not really know what the basic unit of a molecule involved in the true dynamical process is. Thus, the choice of m_0 is somewhat arbitrary; various choices of m_0 simply scale the value of ζ. The fixed quantity is ζ/m_0. Herein we have used $m_0 = m_b$.

The dynamics of a polymer also control its diffusion, so we can also gain insight into these parameters from such measurements. In the reptation model,[2] the diffusion constant, D, for entangled polymers is related to the friction factor by

$$D = \frac{4}{15}\frac{k_B T m_0 M_e}{\zeta M^2} \tag{9}$$

One can then use eq 8 to get values for τ_e from diffusion data.

Comparison with the Data. The data we are reporting here on carefully synthesized ethylene−butene copolymers can clearly be analyzed using eqs 7 and 8 to derive values for τ_e and ζ, as can the literature data we list in Tables 3 and 4. There are many fewer data on polymer diffusion due to the difficulties in such measurements. Losch et al.[30] have obtained diffusion data on a series of hydrogenated polybutadienes of varying branch content using nuclear reaction analysis. Basically, this technique is based on making a thin-film sandwich of a hydrogenous polymer and its deuterated analogue and then

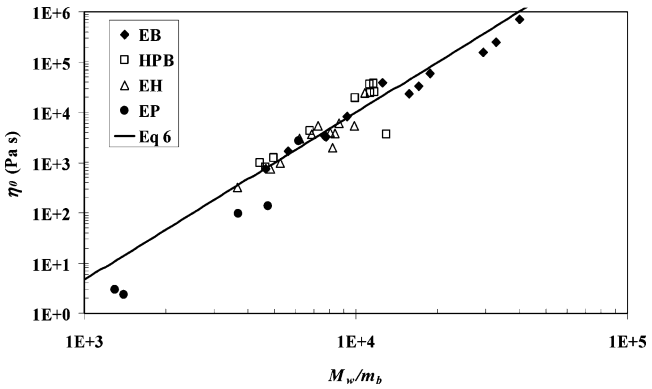

Figure 11. Dependence of zero shear viscosity at 190 °C on number of backbone bonds for a wide range of polyolefins; solid line is from eq 6.

Table 5. Diffusion Data on Hydrogenated Polybutadienes

copolymer	*mf*	*wf*	M_w (kg/mol)	m_b (g/mol)	G_N^0 (kPa)	D (cm^2/s)	M_e (kg/mol)	at 25 °C τ_e (ns)	at 25 °C ζ (Nns/m)	at 190 °C τ_e^{LM} (ns)	at 190 °C ζ (Nns/m)
HPB38	0.23	0.38	103	17.3	1189.7	2.40E−14	1.59	1.53E+04	1.47E+00	7.26E+01	6.96E−03
HPB52	0.35	0.52	85	18.9	867.8	2.50E−14	2.17	5.01E+04	3.11E+00	1.47E+02	9.12E−03
HPB66	0.49	0.66	114	20.9	613.5	5.90E−15	3.07	2.98E+05	1.14E+01	5.42E+02	2.08E−02
HPB75	0.60	0.75	71	22.4	481.3	5.40E−15	3.92	1.60E+06	4.40E+01	2.14E+03	5.89E−02
HPB86	0.75	0.86	85	24.6	349.0	2.30E−15	5.40	6.18E+06	1.09E+02	5.69E+03	1.00E−01
HPB95	0.90	0.95	39	26.7	261.9	6.80E−15	7.20	2.13E+07	2.53E+02	1.45E+04	1.71E−01

determining how long it takes to form a homogeneous single layer. These data were obtained at 25 °C, which we have shifted to 190 °C by using flow activation energies for ethylene−butene copolymers obtained in our labs.[31] These data are summarized in Table 5, where we have also listed the values of τ_e and ζ, derived from eqs 8 and 9. These are plotted with the values derived from our rheological data in Figures 12 and 13.

From a glance at the figures, one can see that there is a monotonic increase in τ_e (and ζ) as the comonomer content increases. This means that there is a general slowing down of the dynamics of these polymers as their degree of branching gets larger. The good agreement between the rheological parameters derived from the metallocene-produced ethylene−butene copolymers and those of the hydrogenated polybutadienes is encouraging. The Miyata data also fit in with the same trends. The diffusion-derived values also agree fairly well, with some discrepancies at high butene content. These differences cold be due to slight errors in the values of flow activation energy we used to extrapolate the room temperature data to 190 °C. Overall, these results give us confidence that a single basic mechanism underlies the dynamics of the saturated hydrocarbon polymers and that the differences between them can be related to their chemical architecture.

We have also looked at how τ_e and ζ depend on m_b, especially because of the correlation of η_0 with m_b that was observed above (eq 5). The correlations here are somewhat tighter than for those on comonomer content, but we must emphasize that we do not have any model of the molecular origins of the observed dependence. One might speculate on such origins (for instance, Losch et al. suggest a dependence on the statistical segment volume[30]), but we do not feel justified in proceeding further at this point. We are now in the process of gathering more data of this kind and will look further into this then.

Combination of Stress Relaxation and Small-Amplitude Oscillatory Shear Experiments. Figure 14 shows typical dynamic data of these ethylene/butene copolymers (EB87), whereby the symbols stand for the data obtained with the small-amplitude oscillatory shear from 10^{-2} to 390 rad/s (this experiment takes ca. 1.5 h). On the other hand, the lines in Figure 14 stand for the dynamic moduli obtained from a 1000 s step strain (stress relaxation) test with 10% strain (linear region) using the following relationships from the theory of linear viscoelasticity for polymer melts:

$$G(t) = \int_{-\infty}^{\infty} H(\lambda) e^{-t/\lambda} \, d \ln \lambda \tag{10}$$

$$G'(\omega) = \int_{-\infty}^{\infty} \left[\frac{H(\lambda)\omega^2\lambda^2}{1+\omega^2\lambda^2} \right] d \ln \lambda \tag{11}$$

$$G''(\omega) = \int_{-\infty}^{\infty} \left[\frac{H(\lambda)\omega\lambda}{1+\omega^2\lambda^2} \right] d \ln \lambda \tag{12}$$

where $G(t)$ stands for the relaxation modulus (experimentally obtained from the step strain test) and $H(\lambda)$ represents the continuous relaxation time spectrum. The software of the Paar Physica MCR500 is very efficient in performing these transformations.

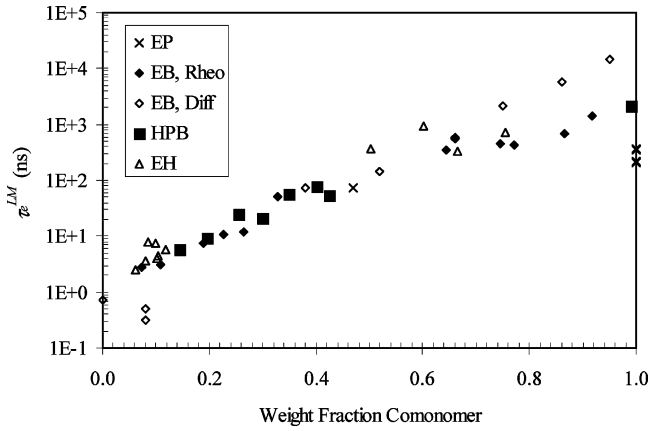

Figure 12. Dependence of the equilibration time on copolymer composition for ethylene−propylene (EP), ethylene−butene (EB), and ethylene−hexene (EH) copolymers.

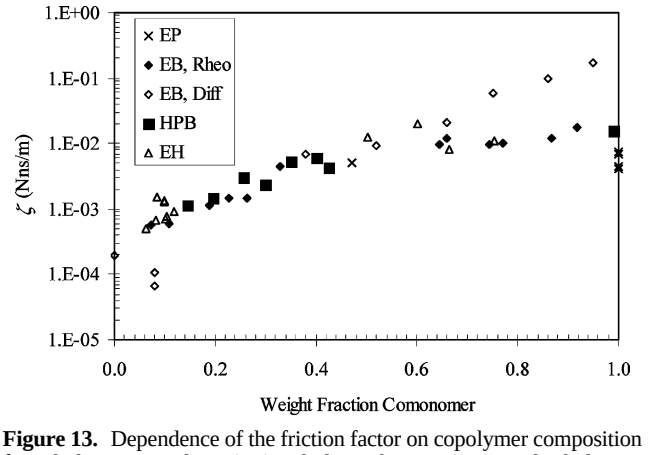

Figure 13. Dependence of the friction factor on copolymer composition for ethylene−propylene (EP), ethylene−butene (EB), and ethylene−hexene (EH) copolymers.

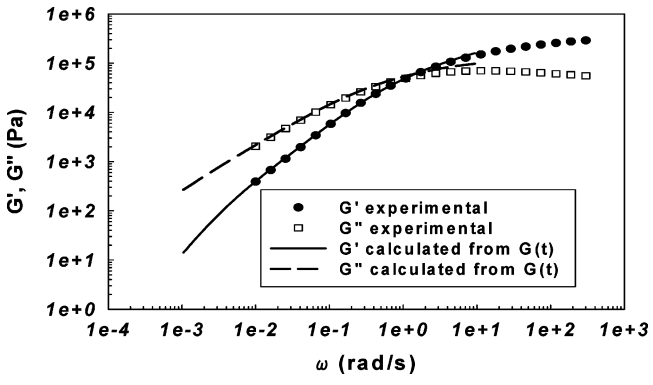

Figure 14. Typical dynamic spectra of an ethylene−butene copolymer (EB87) at 190 °C. Symbols correspond to data measured with small-amplitude oscillatory shear experiment whereas solid lines correspond to the dynamic data calculated from the linear relaxation function measured with a step strain experiment (stress relaxation).

The data in Figure 14 show an excellent agreement between the dynamic data measured with the small-amplitude oscillatory shear (symbols) and the dynamic data calculated from $G(t)$ measured with a step strain experiment over 1000 s, which extends to 10^{-3} rad/s. The relevance of this observation is predicated on the fact that the combination of these tests takes less than 2 h to have the dynamic moduli data from 10^{-3} to ca. 300 rad/s. On the other hand, to cover this frequency range using only small-amplitude oscillatory shear would take ca. 15 h. Consequently, this approach very efficiently extends the experimental frequency window with an extraordinary gain in experimental time when is necessary to extend the small frequency (terminal region) to the 10^{-3} decade.

Conclusions

The method proposed by Fetters and co-workers[11,12] for the calculation of the plateau modulus, G_N^0, based only on the polyolefin chemical structure has been validated by this work on the rheology of well-defined ethylene−butene copolymers. This work also provides scaling relationships between the copolymer composition and various rheological parameters obtainable by robust and relatively fast experimental techniques making these relationships ideally suited for a high throughput experimentation environment as well as the manufacturing plant. Furthermore, this work emphasizes the fundamental character of G_N^0 and η_0 by using them as normalization variables in the construction of "universal master curves" of the linear viscoelastic material functions independent of molecular weight, temperature, and comonomer content. This work also demonstrates that η_0 of these ethylene copolymers depends on the comonomer composition and proposes a new scaling relationship between η_0 and M_w/m_b independent of the comonomer composition, underlining once more the fundamental character of the molecular weight per backbone bond, m_b. There also seem to be correlations of the equilibrium time with m_b. If this holds true universally, this means that very powerful predictive models of polyolefin rheology can be developed solely on the basis of the details of the chemical architecture.

Acknowledgment. The authors express their gratitude to Exxon Mobil Chemical Co. for permission to publish this work and gratefully acknowledge the contributions of M. Amin, B. Brown, G. Capone, and H. Dong to this work. C.A.G.F. benefited from technical discussions with J. Lauger and G. Paroline.

References and Notes

(1) Ferry, J. D. *Viscoelastic Properties of Polymers*, 3rd ed.; Wiley: New York, 1980.
(2) Doi, M.; Edwards, S. F. *The Theory of Polymer Dynamics*; Clarendon Press: Oxford, UK, 1986.
(3) Larson, R. G.; Sridhar, T.; Leal, G. H.; McKinley, A. E.; Likhtman, A. E.; McLeish, T. C. B. *J. Rheol.* **2003**, *47*, 809.
(4) Graessley, W. W. *Adv. Polym. Sci.* **1982**, *47*, 67.
(5) Donald, A. M.; Kramer, E. J. *J. Polym. Sci., Polym. Phys. Ed.* **1982**, *20*, 899.
(6) Donald, A. M.; Kramer, E. J. *J. Mater. Sci.* **1982**, *17*, 1871.
(7) Prevorsek, A. C.; De Bona, B. T. *J. Macromol. Sci., Phys.* **1981**, *B19*, 605.
(8) Prevorsek, A. C.; De Bona, B. T. *J. Macromol. Sci., Phys.* **1986**, *B25*, 515.
(9) Lomellini, P.; Rossi, A. G. *Makromol. Chem.* **1990**, *191*, 1729.
(10) García-Franco, C. A.; Harrington, B. A.; Lohse, D. J. *Rheol. Acta* **2005**, *44*, 591.
(11) Fetters, L. J.; Lohse, D. J.; Richter, D.; Witten, T. A.; Zirkel, A. *Macromolecules* **1994**, *27*, 4639.
(12) Fetters, L. J.; Lohse, D. J.; García-Franco, C. A.; Brant, P.; Richter, D. *Macromolecules* **2002**, *35*, 10096.
(13) Marvin, R. S.; Oser, H. *J. Res. Natl. Bur. Stand.* **1962**, *66B*, 171.
(14) Oser, H.; Marvin, R. S. *J. Res. Natl. Bur. Stand.* **1963**, *67B*, 87.
(15) Carri, G. A.; Winter, H. H. *Rheol. Acta* **1997**, *36*, 330.
(16) Wu, S. *J. Polym. Sci., Polym. Phys. Ed.* **1989**, *27*, 723.
(17) Wu, S.; Beckerbauer, R. *Polymer* **1992**, *33*, 509.
(18) Onogi, S.; Masuda, T.; Kitagawa, K. *Macromolecules* **1970**, *3*, 109.
(19) Masuda, T.; Kitagawa, K.; Inoue, T.; Onogi, S. *Macromolecules* **1970**, *3*, 116.
(20) Van Gurp, M.; Palmen, J. *Rheol. Bull.* **1998**, *67*, 5,
(21) Trinkle, S.; Friedrich, C. *Rheol. Acta* **2001**, *40*, 322.
(22) Trinkle, S.; Walter, P.; Friedrich, C. *Rheol. Acta* **2002**, *41*, 103.
(23) Lohse, D. J.; Milner, S. T.; Fetters, L. J.; Xenidou, M.; Hadjichristidis, N.; Mendelson, R. A.; García-Franco, C. A.; Lyon, M. K. *Macromolecules* **2002**, *35*, 3066.
(24) Harmandaris, V. A.; Mavrantzas, V. G.; Theodorou, D. N.; Kröger, M.; Ramírez, J.; Öttinger, H. C.; Vlassopoulos, D. *Macromolecules* **2003**, *36*, 1376.
(25) Miyata, H.; Yamaguchi, M.; Akashi, M. *Polymer* **2001**, *42*, 5763.
(26) Carella, J. M.; Graessley, W. W.; Fetters, L. J. *Macromolecules* **1984**, *17*, 2775.
(27) Wasserman, S. H.; Graessley, W. W. *Polym. Eng. Sci.* **1996**, *36*, 852.
(28) van Meerveld, J. *Rheol. Acta* **2004**, *43*, 615.
(29) Likhtman, A. E.; McLeish, T. C. B. *Macromolecules* **2002**, *35*, 6332.
(30) Losch, A.; Salomonovic, R.; Steiner, U.; Fetters, L. J.; Klein, J. *J. Polym. Sci., Phys.* **1995**, *33*, 1821.
(31) Mendelson, R. A., internal company data.

MA052581O